International Journal of Engineering

Fused Deposition Modeling of an Aircraft Wing using Industrial Robot with Non-linear Tool Path Generation

S. Harsha Arigela*[a], V. Kumar Chintamreddy[b]

[a] Department of Mechanical Engineering, Jawaharlal Nehru Technological University Anantapuramu, Ananthapur Dt., Andhra Pradesh, India
[b] Department of Mechanical Engineering, N.B.K.R.I.S.T., Vidyanagar, Nellore Dt., Andhra Pradesh, India

P A P E R I N F O	*A B S T R A C T*
	Fused Deposition Modelling (FDM) is an additive manufacturing process to build 3D objects on a horizontal plane from bottom to top. In the conventional FDM process, the printing of curved objects causes the staircase effect and results in poor surface finish. In this work, the FDM process integrated with a 6-DOF Industrial robot is used to print the curved objects by generating non-linear tool paths to avoid the staircase effect. A standard NACA 0015 aircraft wing having curved surfaces is printed without staircase effect at a uniform deposition rate using an industrial robot. The wing is sliced into concentric curved layers either in the form of convex or a concave shape. A new methodology is developed by combining the non-linear toolpaths with the change in extruder orientation to print curved objects at a uniform deposition without any staircase effect. ABB Robotstudio simulation software is used for simulating the printing process and simulation results are validated by printing the portion of the wing using the Industrial robot with an FDM extruder as an end effector. The experimental results showed that the aircraft wing is printed successfully with uniform deposition at constant velocity without any staircase effect.

NOMENCLATURE

FDM	Fused Deposition Modelling	PLA	Polylactide
DOF	Degrees of Freedom	STL	Standard Triangle Language
NACA	National Advisory Committee for Aeronautics	MATLAB	Matrix Laboratory software
CAD	Computer-Aided Design	TCP	Tool Centre Point

1. INTRODUCTION

Fused Deposition Modelling (FDM) is a widely used additive manufacturing technology. It is less expensive compared to other 3D printing processes. FDM machines consist of an extruder (generally having two nozzles) and a horizontal printing bed. The degree of freedom for the conventional FDM machine is limited to three. Those are the movement of the extruder along the X and Y axes, and the movement of the bed along the Z-axis. In the conventional FDM machine, the orientation of the extruder is always perpendicular to the

printing bed and the object is printed in a layered fashion from bottom to top.

The processing steps involved in the conventional FDM process are shown in Figure 1. The first step involved in the FDM process is to generate or create a virtual model or CAD model of the physical object. This CAD model is converted into STL (Standard Triangle Language) format. In the STL format, the entire surface of the object is approximated by triangles. The object in STL format is sliced into horizontal layers based upon the layer thickness. In the third step, the toolpath is generated for each layer in terms of G and M code instructions to the machine to print the desired object. The post-processing step is the removal of support material.

---

*Corresponding Author Email: sriharsha.arigela@gmail.com (S. Harsha Arigela)
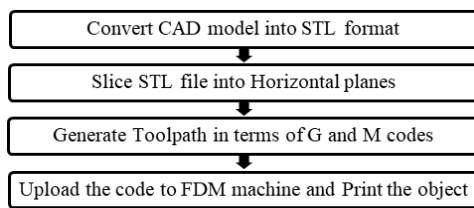
```
┌─────────────────────────────────────────────┐
│   Convert CAD model into STL format          │
└─────────────────────────────────────────────┘
                      ↓
┌─────────────────────────────────────────────┐
│   Slice STL file into Horizontal planes       │
└─────────────────────────────────────────────┘
                      ↓
┌─────────────────────────────────────────────┐
│   Generate Toolpath in terms of G and M codes │
└─────────────────────────────────────────────┘
                      ↓
┌─────────────────────────────────────────────┐
│ Upload the code to FDM machine and Print the object │
└─────────────────────────────────────────────┘
```
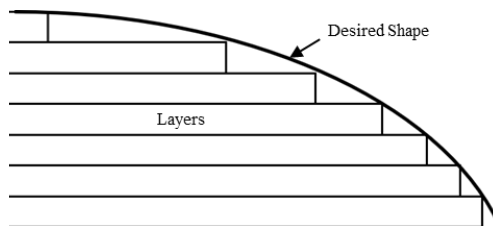
Figure 1. FDM Process

Figure 2. Staircase effect

In a conventional FDM process, while printing the objects with curved surfaces, the staircase effect is one of the common defects. For the curved surfaces, as the material deposition is carried out in layer-by-layer fashion, there is a presence of offset between two adjacent layers as shown in Figure 2. Steps are formed instead of the desired curved shape that results in poor surface finish as shown in the figure.

Tyberg and Bohn [1] developed an adaptive slicing methodology to reduce the staircase effect for curved surfaces. In this method, the slicing thickness is varied throughout along the curved surface. When the curvature is more the slice thickness is reduced to minimize the offset between the adjacent layers and in other cases default layer thickness is considered. The other way to minimize or eliminate the staircase effect is to adopt the non-linear toolpath generation [2]. For the conventional FDM machine, a non-linear toolpath can be generated with the three simultaneous translation movements in x, y, and z directions. But the orientation of the extruder cannot be changed and hence it may lead the extruder to collide with the previously deposited layers during the printing of curved surfaces. At the same time, the extruder's orientation needs to be maintained perpendicular to the printing surface to get homogeneous deposition. Due to the limitation of the orientation using conventional FDM, at some places, the excess of material will be deposited or an inadequate amount of material will be deposited. It results in the variation of part geometry and mechanical properties. Hence the conventional FDM machines are not suitable to produce uniform deposition of curved surfaces due to the limitation of extruder orientation. Shembekar et al. [3] proposed a collision-free trajectory planning for printing using a non-planar deposition. It indicated that collision with the printing surface can be avoided by properly controlling the trajectory parameters with

respect to surface curvature. The proposed approach is implemented by using a 6-DOF robot arm. STL files of non-planar surfaces were generated with information of unit normal vectors set and the information on vertices of each triangle in 3D Cartesian coordinates. By projecting this data on the 2D Cartesian coordinate plane, the shape of the projected surface is obtained. In this way, all the surfaces (slices) were obtained for the 3D structure. Complex 3D structures with various curvatures like Curved beam, Mini armor chest protector, Wind turbine blade, Mini Car Bonnet were successfully fabricated using the proposed collision-free trajectory and a satisfactory surface finish is accomplished. Bhatt et al. [4] proposed a robotic cell for multi-resolution AM (Additive manufacturing with two different nozzle sizes). The proposed cell consists of two 6 degrees of freedom (DOF) robot manipulators. Algorithms were developed for decomposing parts into multi-resolution layers and generating collision-free trajectories for these robot manipulators. Euclidean distance transform (EDT) based layering algorithm is used to generate non-planar layers required for printing. EDT is used to construct the 3D transform distance from the 2D transform distance. Sample specimens like Mini car bonnet, Mini airplane wing, Composite slider, and Helix shape slider were printed with non-planar layers for the exterior regions with the ABB IRB 120 robot. The planar layers were printed for the interior regions of those specimens with the ABB IRB 2600 robot. While printing the airplane wing with the proposed slicing technique, non-planar layers for the outer region and planar layers for the inner region were generated. This will eliminate the staircase effect but the mechanical properties of the wing will be the same just like the same wing printed with the conventional FDM process. Jensen et al. [5] introduced two new deposition-strategies for 5 DOF (five degrees of freedom) and 6 DOF extrusion-based additive manufacturing (AM) process. The 5 DOF extrusion-based additive manufacturing strategy is called the tool path projection approach. This approach was inspired by the texturing of 3D bodies used in computer-generated imagery (CGI) for generating layers. This approach follows a sequence in which the surface of the geometry is unwrapped, and in its flattened form, texturized, and then the geometry is wrapped back to its 3-dimensional shape. This is done for each layer. The 6 DOF extrusion-based additive manufacturing strategy is called parent-child-approach. This approach allows local features of the workpiece to be built in different directions by reorienting the workpiece accordingly, exploiting the 6DOF of the system. It indicated that the proposed automated tool path projection method to generate concentric shell layers as a remedy for the staircase effect. Ishak et al. [6] integrated six degrees of a freedom robot arm with a fused deposition modeling

system for multi-plane and 3D lattice structure printing applications. The proposed system has the advantage of printing in multiple planes over a conventional Cartesian 3D printer platform which is limited to single-plane layering for the printing of 3D objects. 3D lattice structures and an object with an overhang structure were printed with the proposed platform. Ahlers et al. [7] presented a slicer (slices generating algorithm) that is capable of generating non-planar toolpaths from any object to avoid the staircase effect. In this work, first object is sliced with the regular layer generation to generate the planar layers. And then the top and shell areas are removed and replaced by nonplanar layers to generate the needed space for the nonplanar extrusions. The replacement is done by first finding the layer where the nonplanar surface should be generated. In this way, nonplanar layers are generated. Collision prevention while printing nonplanar layers is also taken care of in the proposed printing approach. The objects printed with the nonplanar layers by the proposed approach have shown better surface quality compared with objects printed with conventional planar layers. Kubalak et al. [8] have presented a multi-axis toolpath generation algorithm and it is implemented on a 6-DOF robotic arm ME (Material Extrusion) system to fabricate tensile specimens at different global orientations. ABS tensile specimens at various inclination angles were printed using the proposed multi-axis technique. The results showed that the multi-axis specimens had similar performances regardless of orientation and were equivalent to the 3-DOF specimens printed with the conventional FDM machine. Balogun et al. [9] developed a generic electrical energy model for the 3D printing process and indicated the warm-up time for the FDM machine is considerably high and suggested that energy efficiency can be improved without cooling down the 3D printer to room temperature before the next part is printed. Kumar et al. [10] examined the tribological behaviour of Ultra High Molecular Weight Polyethylene (UHMWPE) and Polyether ether ketone (PEEK) biopolymers which are mostly used for prosthesis used in Total Knee Replacement (TKR). The test specimens were fabricated using Direct Laser Metal Sintering (DMLS) and indicated that PEEK is a suitable material for TKR due to less wear rate compared to the UHMWPE. Kumar et al. [11] developed a robotic manipulator to recognize the speech and n write letters by using a pen as an end effector. In this work, a dynamic time warping (DTW) algorithm is used for recognizing the sound signal and to generate the executable command to move the robot in its workspace. Moradi et al. [12] statistically analysed 3D printing of PLA (Polylactic acid) by the Fused Deposition Modelling process. The honeycomb pattern is selected in this work for infill. It indicated that layer thickness is the major control variable. It also indicated

that the infill percentage and extruder's temperature had a significant influence on the tough fracture of printed parts. Moradi et al. [13] investigated the influence of layer thickness, infill percentage, and extruder temperature on the failure load, thickness, and build time of bronze polylactic acid (Br-PLA) composites 3D printed by the fused deposition modeling (FDM). The failure load and build time were considered as objective functions. In this work, a comparison was made between PLA and Br-PLA in terms of failure load. Moradi et al. [14-17] investigated the post-processing of 3D printed PLA (polylactic acid) parts. To remove the defects of workpieces printed by the FDM process, a post-processing operation is introduced in this work that uses a low power CO_2 laser. Optimum values of the process parameters were obtained in this work from the DOE analysis.

In the FDM process, an alternative slicing technique is needed to generate nonplanar layers for objects having curved surfaces to eliminate the staircase effect. In the conventional FDM machine, due to limited degrees of freedom (3), it is not possible to print the curved objects without staircase effect. The objective of the present work is to develop a new slicing methodology to print the objects having curved surfaces without staircase effect using the Industrial robot. The curved surface object is sliced into nonplanar layers that are concentric to the shape of the object. These nonplanar layers are printed by generating non-linear toolpaths using the Industrial robot with an FDM extruder as the end-effector. To obtain uniform and homogeneous deposition along the nonplanar layers, the extruder needs to move with constant velocity and its orientation needs to be maintained perpendicular to printing surfaces. The proposed methodology is applied to print a segment of an aircraft wing having NACA 0015 [18] Airfoil shape. The NACA aircraft wings are developed by the National Advisory Committee for Aeronautics [18]. Data for these Airfoil shapes are available on the UIUC Airfoil Coordinates Database [19]. Simulation of the extruder's movement along the generated toolpath is carried out in ABB Robotstudio software for validation. The simulation results showed that there is no presence of singularity errors and the generated toolpath is within the range of the robot's workspace. The actual printing of the aircraft wing is done successfully without the staircase effect. The methodology followed in slicing and printing the segment of the aircraft wing is presented in this paper.

2. METHODOLOGY

2. 1. Nomenclature of the Wing   A wing is a type of fin that produces lift force to fly while moving through the air [20]. The wing has curved surfaces on

the upper and the lower portions, designed to give an adequate ratio of lift to drag. The cross-sectional shape of a wing is called Airfoil. Wings are classified as symmetric and asymmetric Airfoil-shaped wings. Figure 3 shows the nomenclature of an asymmetric Airfoil-shaped wing and Figure 4 shows the nomenclature of a symmetric Airfoil-shaped wing. The lower surface of the wing is subjected to higher static pressure compared to the upper surface. The lift force is generated due to the pressure difference between these two surfaces of the Airfoil. The leading edge is situated at the front part of the Airfoil and it has maximum curvature. The trailing edge is situated at the rear part of the Airfoil. These two edges are connected by a straight line called chord line. Angle "α" is called the angle of attack that is measured between the direction of the relative wing and chord line. The camber line is constructed by joining the locus of points midway between the upper and lower surfaces. If the Airfoil is symmetric, then both the camber line and the chord line will coincide. In this work, the symmetric Airfoil NACA 0015 [18] wing is selected for printing.

2. 2. Selection of Aircraft Wing's Orientation for Slicing

In this work, a symmetric Airfoil-shaped wing as shown in Figure 4 is selected for printing using the Industrial robot. In the conventional FDM process, the wing can be sliced into three possible ways with respect to two reference planes viz. "S" and "R" as shown in Figure 5.

The reference plane "R" is considered as a plane parallel to the flat base of the wing as shown in Figure 5. Another reference plane "S" is considered as a plane containing the chord lines and perpendicular to the reference plane "R".
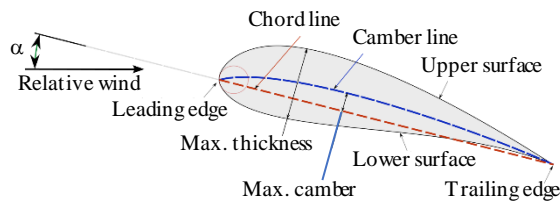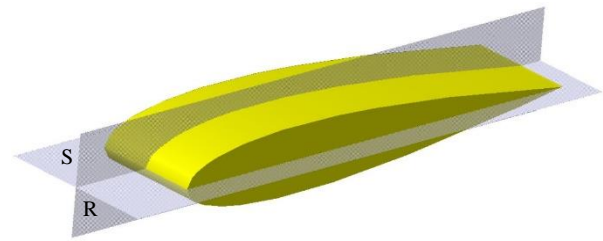

Figure 5. A portion of the wing with plane "S" passing through chord line and plane "R" parallel to the wing base

For conventional FDM, the selected aircraft wing can be sliced and printed in three possible orientations with minimum support structure with reference to planes "R" and "S" as shown in Figure 6, Figure 7 and Figure 8. In all these three cases, slicing is carried out with a plane parallel to the horizontal printing bed. The boundaries (shells) for each of these layers are shown in red color and the infill is shown in yellow color for these three cases as shown in Figures 6, 7 and 8.

In the first orientation, as shown in Figure 6, the slicing is carried out parallel to plane "S" and perpendicular to plane "R". In this orientation the cross-sectional area of each sliced layer is different and it produces the staircase effect. Due to variation in the cross-sectional area of each layer, the object may not have uniform strength. In this orientation, the support structure is required to build the wing up to the chord length's height.
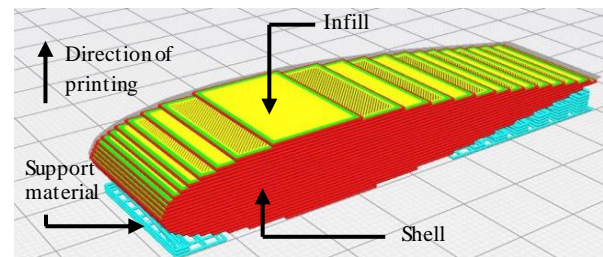

Figure 3. Airfoil Nomenclature (asymmetric type) [17]

Figure 6. Case 1: Slicing perpendicular to plane "R" and parallel to plane "S"

Figure 4. NACA 0015 (Symmetric type Airfoil) [18]
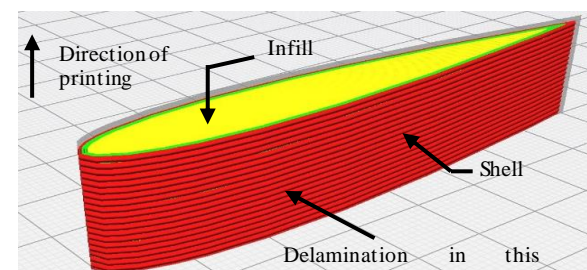

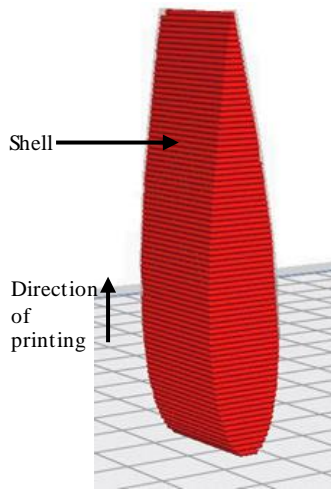**Figure 7.** Case 2: Slicing perpendicular to plane "S" and parallel to plane "R"

Figure 8. Case 3: Slicing perpendicular to both plane "R" and plane "S"

In the second orientation, as shown in Figure 7, the slicing is carried out perpendicular to plane "S" and parallel to the plane "R". In this orientation, the objects can be printed without staircase effect and support structure but the tensile strength is poor along the direction of printing. Zhao et al. [21] studied the tensile strength and elastic property of PLA material printed with different angles and layer thicknesses through the FDM process. It indicated that the tensile strength and Young's modulus of PLA specimen increased with the increase in the printing angle or decrease in layer thickness. It also indicated that the specimen printed at 0^0 angle (i.e. layers are parallel to tensile load direction) having comparatively less tensile strength compared to specimen printed at other angles (15°, 30°, 60°, 90°). At 90° the printed layers are perpendicular to tensile load direction. Moreover, in this orientation, the aircraft wing will suffer a serious delamination effect due to the action of high static pressure (load) on the lower surface. Perkowski [22] indicated that the part printed by the FDM process with PLA material will fail, if it is subjected to the compressive load applied perpendicular to the direction of printing due to the buckling of layers. This is caused by the layers delaminating and bending out of the plane of the applied stress.

In the third possible orientation, as shown in Figure 8, the slicing is carried out perpendicular to both plane "R" and plane "S". In this case, the support structure is required to build up to the maximum thickness of the wing. The major drawback of this orientation is that the staircase effect and poor tensile strength along the direction of printing. The cross-section of each layer is not uniform and the wing may not have uniform strength.

In the present work, a new methodology is adopted for slicing and printing of the wing as shown in Figure 9 using the Industrial robot. The slicing is carried out

parallel to the outer curved surfaces of the wing i.e. in the concentric form. In this orientation, the support structure is required up to the chord line's height. In this slicing method, each layer is having maximum surface area contact to adjacent layers and results in comparatively higher strength in perpendicular directions along the curved surfaces than the conventional orientations as shown in Figures 6, 7 and 8. This slicing method also avoids staircase effect. For the support structure, the slicing is carried out in a conventional horizontal slicing, and to eliminate the staircase effect in the lower surface of the wing two nonplanar layers are required as shown in Figure 9. The layers of the support structure are represented in red color and the layers of the wing are represented in green color as shown in Figure 9. Due to limited degrees of freedom, in the conventional FDM machine, the change in orientation of the extruder is not possible to print the nonplanar layers that are shown in Figure 9. The layers in this orientation have stronger bonding and minimum delamination due to nonplanar type and maximum surface area contact.

The relative merits and demerits of the mentioned slicing methodologies and orientations are shown in Table 1.
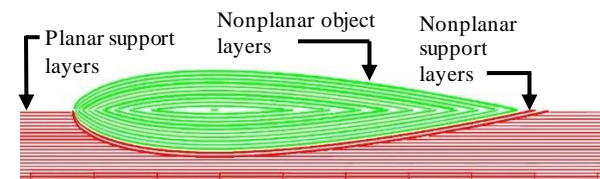

Figure 9. Slicing along the contour of the wing (nonplanar slicing)

TABLE 1. Relative merits and demerits of slicing

	Case 1 Figure 6	Case 2 Figure 7	Case 3 Figure 8	Slicing along the contour of the wing Figure 9
Staircase effect	Yes	No	Yes	No
Strength	Moderate	Poor	Poor	High
Slicing	Linear	Linear	Linear	Both Linear and Non-Linear
Printing with Conventional FDM	Possible	Possible	Possible	Not possible
Extruder's Orientation when printing	No Change	No Change	No Change	Changes when printing nonplanar layers
Support structure	Required	Not Required	Required	Required
Type of support structure	Planar Layers	Not Required	Planar Layers	Both planar and non-planar layers

2. 3. Steps Involved in Printing the Aircraft Wing using Industrial Robot   In this work, the aircraft wing is printed with an Industrial robot using the extruder as an end effector. In this work, a small segment of the wing is printed. Various steps involved in printing the aircraft wing [18] are presented in this section and they are 1) Layer generation 2) Toolpath generation 3) Simulation of Printing in ABB Robotstudio software and 4) Printing using the Robot.

2. 3. 1. Layer Generation   The data points for the lower surface and upper surface of the Airfoil of NACA 0015 [18]   wing are shown in the following Table 2. Data for this Airfoil shape is taken from the UIUC Airfoil Coordinates Database by considering the value of chord length as 80 mm.

1. Based on the data points, two splines are fitted for both the lower surface and upper surface respectively. The obtained Airfoil shape or cross-section of the wing is shown in Figure 10. These two splines are considered as base splines.

2. Normal vectors at discrete intervals (0.5 mm) to the lower base spline are generated. The direction of each normal vector is reversed (towards the chord line) and the obtained vectors for the base spline are shown in Figure 11.

3. On each obtained vector, a new point is determined at a certain distance from the origin of the respective vector towards the chord line. This distance is equal to the layer thickness. The layer thickness considered in this work is 0.5 mm. Again, one more spline is fitted through the newly obtained points. Figure 12 shows the newly obtained spline over the base spline that is separated by 0.5 mm.

4. By repeating the above step and by considering the distance as multiples of 0.5 mm, new splines are created. The extended portion of each spline beyond the chord length is trimmed off. Following the same procedure for the upper surface, concentric splines are generated. Figure 13 shows the final set of splines that are obtained for the cross-section of the wing.

5. From the obtained set of splines, each spline is swept along a line segment towards the depth direction to generate a layer. All the splines are swept in the same way to generate a set of layers. Figure 14 shows a generated layer obtained by sweeping a spline.

Figure 10. Airfoil Shape

Figure 11. Vectors along the Lower surface

Figure 12. New obtained spline above the Base spline

Figure 13. Set of splines

Figure 14. Generated layer

TABLE 2. Data Points [18]

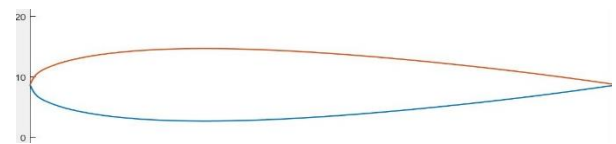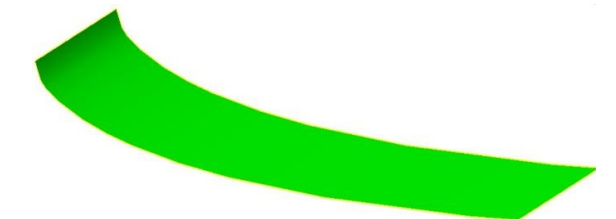| S. No.	Lower Surface		Upper Surface	
	X	Z	X	Z
1	15	8.7016	15	8.7016
2	16	6.808	16	10.5952
3	17	6.0872	17	11.316
4	19	5.1472	19	12.256
5	21	4.5016	21	12.9016
6	23	4.0192	23	13.384
7	27	3.356	27	14.0472
8	31	2.964	31	14.4392
9	35	2.76	35	14.6432
10	39	2.7	39	14.7032
11	47	2.8984	47	14.5048
12	55	3.408	55	13.9952
13	63	4.1384	63	13.2648
14	71	5.0376	71	12.3656
15	79	6.0784	79	11.3248
16	87	7.2536	87	10.1496
17	91	7.8952	91	9.508
18	95	8.5752	95	8.828

2. 3. 2. Toolpath Generation   The sliced layers of the aircraft wing consist of concave shapes below the chord line and convex shapes above the chord line. To print the concave-shaped layers below the chord line need supporting structure. The support structure consists of both planar (flat) and non-planar (curved) type of layers. Two concave-shaped layers were generated to support the aircraft wing's bottom layer to eliminate the staircase effect at the bottom portion. After completion of printing the aircraft wing, the entire support structure is removed. The cross-sectional view of the aircraft wing with support structure is shown in Figure 15. In the figure, it can be observed that a support structure having nonplanar layers are used at the lower surface of the aircraft wing in order to eliminate the staircase effect. 3D view of the aircraft wing is shown in Figure 16. In this work, both wing and support structure are printed using a robot and the tool path is generated separately for both support structure and wing.

For printing the portion of the support structure with flat horizontal layers, a CAD model up to that portion is developed based on data points shown in Table 2. In this work, a chord line length of 80 mm is considered. The width of the wing segment is considered as 20 mm. The CAD model is converted into STL format and it is sliced into horizontal layers as shown in Figure 17.
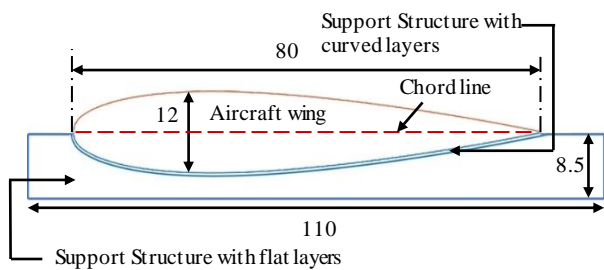

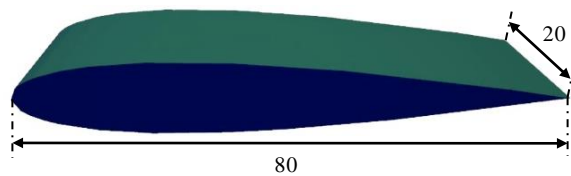**Figure 15.** The cross-sectional view of the aircraft wing with the support structure

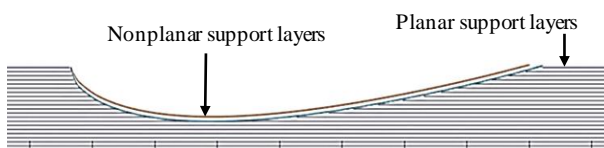**Figure 16.** 3D view of the aircraft wing

Figure 17. Front view of the slices of support

Each layer's toolpath is generated in a zig-zag fashion based upon the scan-line polygon filling algorithm [23]. The fill density of the support structure is taken as 50% to save the material and time and for ease of cleaning. The toolpath is converted into rapid commands (MoveL) for the ABB Industrial robot to print the support structure. For generating the two curved (concave-shaped) layers of the support structure, the proposed layer generation technique in the above section is used. The toolpath generation for these two layers is similar to the aircraft wing's layers, which is explained in the remaining part of this section.

The tool path for printing the wing is generated by combining the non-linear motion of the robot wrist combined with continuous change in orientation. As shown in Figure 11, the set of layers were generated by sweeping the splines. In generating non-linear toolpath for each layer, the extruder needs to move in all the x, y and z coordinates simultaneously. At the same time, the orientation of the extruder needs to vary to maintain perpendicular orientation to layer to get uniform deposition and to avoid collision with the previously printed layers. The maximum rotation (roll) along the x-axis considered in this work is $\pm 45^0$. Figure 18 shows the schematic view of the tool (Extruder) moving along a nonplanar layer in a nonlinear fashion keeping the orientation perpendicular to the layer. The extruder keeps on changing the orientation along with the movement at constant velocity to facilitate homogeneous deposition of material as shown in the figure.

Two types of toolpaths that are considered alternatively for generating the toolpaths while depositing the material along the curved layers. A MatLab program is developed to generate these toolpaths. This MatLab program takes the coordinates on the layer as input and joins them logically to create the path. If the tool is required to move from the first coordinate to the second coordinate, the MatLab program generates the output in the form of MoveL (rapid code for the robot) statement which will make the robot move from the first coordinate to the second coordinate in a linear fashion. In this way, the toolpath is created for the entire layer. The first type of the toolpath is generated in such a way that the tool moves along the curved layer (treating the movement along the y-axis) and changes its orientation while moving from
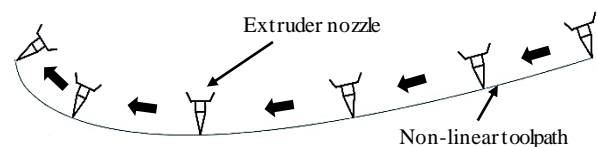

Figure 18. Schematic view of the tool moving along a curved layer

one position to another. This movement is incremented along the other axis (x-axis) for generating the toolpath for that layer. The isometric view of this type of toolpath is shown in Figure 19. Schematically the toolpath is drawn along the layer in Figure 19 for representation purpose. The top view of the actual toolpath is shown in Figure 20.

The second type of toolpath is generated by changing the direction of the movement of the extruder is along the depth direction (x-axis) with constant orientation. This movement is incremented towards the curve (towards the y-axis) by changing the orientation for each increment. The isometric view of this toolpath is shown in Figure 21. Schematically the toolpath is drawn along the layer in Figure 21 for representation purpose. The top view of the actual toolpath is shown in Figure 22.

These two types of toolpaths are used alternatively for consecutive layers to produce stronger bonds between layers and result in an increase in the strength of the wing. For the outer layers of the wing, the first type of toolpath is used for printing to avoid the staircase effect.
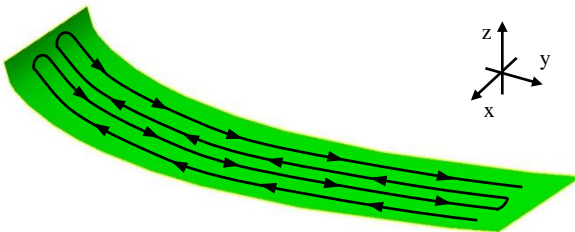

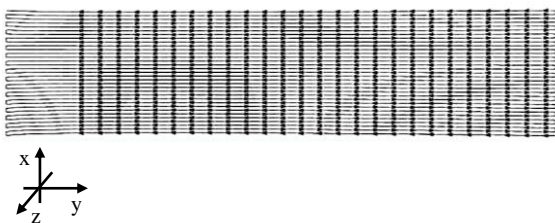**Figure 19.** Isometric view of Toolpath type 1
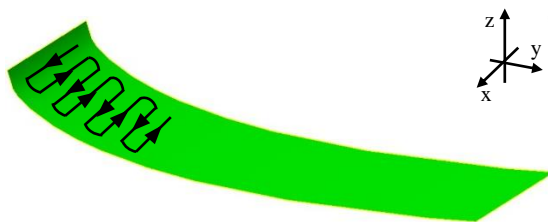

Figure 20. Top view of Toolpath type 1

Figure 21. Isometric view of Toolpath type 2
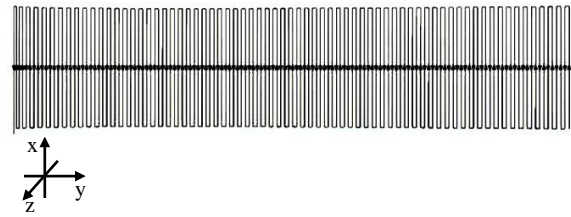

Figure 22. Top view of Toolpath type 2

2. 3. 3. Simulation of Printing in ABB Robotstudio Software

In this work, ABB make IRB 1600 robot acts as a fused deposition modeling machine with a higher degree of freedom (6) by attaching the extruder as an end effector. Before carrying out the actual printing process, simulation of the toolpath movement is done in ABB Robotstudio simulation software for validation. This simulation is helpful for checking out the presence of any singularity errors. This can be also useful to check whether all the positions were within the reach of the robot or not. For simulation, a model of the extruder is built and attached to the IRB 1600 robot and it acts as a tool. The tip of the nozzle is defined as the TCP (Tool Centre Point).

2. 3. 4. Printing using the Robot

A dual nozzle extruder is attached to the flange of the ABB IRB 1600 robot's wrist to facilitate Fused deposition modeling. TCP (Tool Centre Point) is defined at the tip of nozzle 1. This setup is shown in Figure 23.

The toolpath that has been generated in terms of Rapid commands is given as input to the ABB IRC5 controller. These rapid commands do contain both motion instructions and digital output signals. The motions instructions in the form of MoveL (Move Linear) are used to control the movement of the robot. As the TCP (Tool Centre Point) is defined at the tip of the nozzle, the nozzle follows the defined toolpath.

Figure 23. Extruder attached to the robot

The other rapid commands are digital output signals. These signals are being used to control material deposition. Here the material used for printing is PLA (Polylactic acid) with a melting point of 195^0. This digital output signal is in binary form i.e. either 0 or 1, a simple off or on. The digital output signal is fed to the Arduino Uno board's digital input pin. Here the Arduino board does contain an L293D Motor Driver for stepper motor control. A program is dumped into this Arduino board to rotate the stepper motor at specific constant rpm if the digital output from the controller is 1. This rotation is only in one direction. If the digital output signal is 0, the stepper motor stops rotating and holds its position. When the stepper motor is in ON state, the material in the form of wire will pass through the heat block and gets melted and gets deposited through the nozzle. Once the material leaves the nozzle and gets exposed to the atmosphere, it gets solidified instantly within 0.1s. These digital output signals are passed logically so that wherever there is a need the material gets deposited in between two specific points along the toolpath. If not, the material won't get deposited. In this way, the stepper motor will be controlled. Process parameters that were considered for the FDM process in this work are shown in Table 3. Layer thickness is one of the important process parameters for the FDM process. Total printing time is also affected by layer thickness. In this work, is used to print layers of thickness 0.5 mm and deposition speed i.e TCP (Extruder's nozzle tip) speed is considered to be 40 mm/s. Infill density for support is considered as 50%. This will ensure the easy removal of the support structure after the printing process is completed. The aircraft wing is printed with 100% infill density. The extrusion temperature is maintained at 195^0 C. This is done by using Arduino Atmega 2560 board and Ramps 1.4 Shield. All the time there is continuous feedback from the heat block to maintain a constant temperature. To take away excessive heat from the nozzle's heat block, a cooling fan is also being controlled by this Arduino board. Using this same feedback system the bed temperature is also maintained at 70^0 C.

TABLE 3. Process parameters

S. No	Process Parameter	Value
1	Layer Thickness (For both planar and nonplanar layers)	0.5 mm
2	Deposition speed	40 mm/s
3	Infill density for support	50%
4	Infill density for aircraft wing	100%
5	Nozzle Diameter	0.5 mm
6	Extrusion Temperature	195^0
7	Bed Temperature	70^0

The relative advantage of the methodology adopted to print the aircraft wing in this work over and the methodology adopted by Bhatt et al. [4] is shown in Table 4.

3. RESULTS AND DISCUSSION

Simulation is carried out in Robotstudio software to check the movement of the tool along the defined toolpath. The generated toolpath in the form of rapid commands is uploaded to the software environment. The movement of the tool speed is maintained at 40 mm/s. Simulation is carried out in two stages. In the first stage, the simulation of the tool moving along the toolpath for the support is checked. For this movement, the tool remains in the same perpendicular orientation to the planar toolpath throughout the simulation with a movement speed of 40 mm/s. Tool moving along the two nonplanar layers in the support structure is also simulated in this stage at the same speed but with a change in the tool's orientation. The toolpath generated in the robotstudio simulation environment for the support is shown in Figure 24.

In the second stage, the simulation of the tool moving along the toolpath for the wing segment is checked. In this movement, the tool changes its orientation perpendicular to the non-linear toolpath throughout the simulation with a movement speed of 40 mm/s. The toolpath generated in the robotstudio simulation environment for the aircraft wing segment is shown in Figure 25.

TABLE 4. Relative advantages of the present methodology

	Aircraft wing printed through proposed methodology in this work	Aircraft wing printed through the methodology presented by Bhatt et al. [4]
Type of layers used to print the aircraft wing	Non-planar layers only	Both planar and nonplanar layers
Type of slicing	Based on Splitting the part into a set of splines	Based on Euclidean distance transform
Nozzle diameter	0.5 mm	0.4 mm and 0.8 mm
Robot end effector velocity	40 mm/s	25 mm/s
Number of Robots used	1	2

Figure 24. Toolpath for the support

Figure 25. Toolpath for the Aircraft wing segment

The simulation results showed that the TCP (tip of the nozzle) followed the toolpath with desired orientations at every position without singularity errors. All the positions are within reach. Hence the generated toolpath for both the support and wing segment is validated.

After validating the simulation results, the printing of the segment of the NACA 0015 [18] Airfoil shaped wing is carried out successfully with the robot without any singularity errors. The tip of the extruder reached every desired position with the corresponding orientation. Figure 26 shows the printed model with the support structure. Black-colored PLA is used to print the aircraft wing and yellow-colored PLA is used to print the support structure.

Thermal stresses will be induced as the non-planar surfaces were printed. This results in warping of the support structure. To eliminate this warping Thermo plasters (acts like fixtures) were used to fix the position of the support before printing the wing segment. The support structure is removed once the printing of the wing segment is completed. The aircraft wing printed through this proposed slicing method will have good mechanical properties compared to the aircraft wing printed with both planar and nonplanar layers through the methodology presented by Bhatt et al. [4]. Voids will be created between planar and nonplanar layers if the aircraft wing is printed through the methodology developed by Bhatt et al. [4]. This can be overcome by adopting the slicing technique presented in this paper.

One of the major drawbacks of conventional FDM machine is that it produces staircase effect while printing curved surfaces. Therefore, rough surfaces are obtained. This is due to the limited degree of freedom of the FDM machine. The orientation of the extruder remains the same throughout the printing process. If the orientation doesn't change, the homogeneous distribution of the material is not possible while printing is carried out over curved surfaces. Hence a higher degree of freedom machine is required to change the orientation of the robot. Nonplanar layers are supposed

to be generated instead of conventional planar layers to eliminate the staircase effect. A six-axis industrial robot is considered in this work to meet the requirement. Non-planar layers were generated based upon the proposed nonplanar layer generating strategy and toolpath is generated for these layers with the extruder having a perpendicular orientation with respect to the surface to get the homogeneous distribution of the material. After validating the simulation results, the printing of the Airfoil shaped wing is carried out successfully.

4. CONCLUSIONS

1. In this paper, a new nonplanar layer generating strategy is developed and it is applied to a NACA 0015 [18] aircraft wing to generate nonplanar layers along the curved surface. Printing is done by using the extruder as the end effector of the robot.
2. The staircase effect, the major drawback of the conventional FDM process can be overcome by making use of the Industrial robot's extra degree of freedom by adopting the proposed layer generating and printing strategy, and hence good surface finish is obtained.
3. Homogenous deposition of material along the non-linear toolpaths is possible through the continuous change of the extruder's orientation with the help of the robot, which can't be done in the conventional FDM process.
4. Future work can be focused on generating toolpaths for the wing segment with a variable cross-sectional area along the depth direction.

5. REFERENCES

1. Tyberg, J. and Bøhn, J. H., "FDM systems and local adaptive slicing", *Materials & Design,* Vol. 20, No. 2, (1999), 77-82, DOI: 10.1016/S0261-3069(99)00012-6.

2. Gibson, I., Rosen, D. W. and Stucker, B., "Additive Manufacturing Technologies", Springer, (2010), ISBN: 978-1-4419-1119-3.

3. Shembekar, A. V., Yoon, Y. J., Kanyuck, A. and Gupta, S. K., "Trajectory Planning for Conformal 3d Printing Using Non-Planar Layers", ASME 2018 International Design Engineering Technical Conferences and Computers and Information in Engineering Conference IDETC/CIE, Quebec City, Quebec, Canada, (August 26-29, 2018), DOI: 10.1115/DETC2018-85975.

4. Bhatt, P. M., Kabir, A. M., Malhan, R. K., Shah, B., Shembekar, A. V., Yoon, Y. J. and Gupta, S. K., "A Robotic Cell for Multi-Resolution Additive Manufacturing", International Conference on Robotics and Automation (ICRA), Montreal, QC, Canada, (2019), 2800-2807, DOI: 10.1109/ICRA.2019.8793730.

5. Jensen, M.L., Mahshid, R., D'Angelo, G., Walther, J.U., Kiewning, M.K., Spangenberg, J., Hansen, H.N. and Pedersen, D.B., "Toolpath Strategies for 5DOF and 6DOF Extrusion-Based Additive Manufacturing", *Applied Sciences,* Vol. 9, No. 19, (2019), DOI: 10.3390/app9194168.

Figure 26. Printed Aircraft wing

6. Ishak, I. B. and Larochelle, P., "MotoMaker: a robot FDM platform for multi-plane and 3D lattice structure printing", *Mechanics Based Design of Structures and Machines,* Vol. 47, No. 6, (2019), 703-720, DOI: 10.1080/15397734.2019.1615943.

7. Ahlers, D., Wasserfall, F., Hendrich, N. and Zhang, J., "3D Printing of Nonplanar Layers for Smooth Surface Generation", IEEE 15th International Conference on Automation Science and Engineering (CASE), Vancouver, BC, Canada, (2019), 1737-1743, DOI: 10.1109/COASE.2019.8843116.

8. Kubalak, J. R., Wicks, A.L. and Williams, C. B., "Exploring multi-axis material extrusion additive manufacturing for improving mechanical properties of printed parts", *Rapid Prototyping Journal,* Vol. 25, No. 2, (2019), 356-362, DOI: 10.1108/RPJ-02-2018-0035.

9. Balogun, V. A. and Oladapo, B. I., "Electrical Energy Demand Modeling of 3D Printing Technology for Sustainable Manufacture", *International Journal of Engineering, Transactions A: Basics,* Vol. 29, No.7, (2016), 954-961, DOI: 10.5829/idosi.ije.2016.29.07a.10.9.

10. Sandeep Kumar, Y., Rajeswara Rao, K .V. S. and Sunil, R. Y., "Investigation of Wear Behavior of Biopolymers for Total Knee Replacements Through Invitro Experimentation", *International Journal of Engineering, Transactions B: Applications,* Vol. 33, No. 8, (2020), 1560-1566, DOI: 10.5829/ije.2020.33.08b.14.

11. Manoj Kumar, V. and Srii Hari Thipesh, D., "Robot Arm Performing Writing through Speech Recognition Using Dynamic Time Warping Algorithm", *International Journal of Engineering, Transactions B: Applications,* Vol. 30, No. 8, (2017), 1238-1245, DOI: 10.5829/ije.2017.30.08b.17.

12. Moradi, M., Meiabadi, S. and Kaplan, A., "3D Printed Parts with Honeycomb Internal Pattern by Fused Deposition Modelling; Experimental Characterization and Production Optimization", *Metals and Materials International,* Vol. 25, No. 5, (2019), 1312–1325, DOI: 10.1007/s12540-019-00272-9.

13. Moradi, M., Karami Moghadam, M., Shamsborhan, M. and Bodaghi, M., "The Synergic Effects of FDM 3D Printing Parameters on Mechanical Behaviors of Bronze Poly Lactic Acid Composites", *Journal of Composites Science,* Vol. 4, No. 1, (2020), DOI: 10.3390/jcs4010017.

14. Moradi, M., Karami Moghadam, M., Shamsborhan, M., Bodaghi, M. and Falavandi, H., "Post-Processing of FDM 3D-Printed Polylactic Acid Parts by Laser Beam Cutting", *Polymers,* Vol. 12, No. 3, (2020), DOI: 10.3390/polym12030550.

15. Moradi, M. and Karami Moghadam, M., "High power diode laser surface hardening of AISI 4130; statistical modelling and optimization", *Optics & Laser Technology,* Vol. 111, (2019), 554-570, DOI: 10.1016/j.optlastec.2018.10.043.

16. Moradi, M., Moghadam, M. K., Shamsborhan, M., Beiranvand, Z. M., Rasouli, A., Vahdati, M., Bakhtiari, A. and Bodaghi, M., "Simulation, statistical modeling, and optimization of CO2 laser cutting process of polycarbonate sheets", *Optik*, Vol. 225, (2021), DOI: 10.1016/j.ijleo.2020.164932.

17. Moradi, M., Falavandi, H., Moghadam, M. K. and Shaikh Mohammad Meiabadi, M., "Experimental Investigation of Laser Cutting Post Process of Additive Manufactured Parts of Poly Lactic Acid (PLA) by 3D Printers Using FDM Method", *Modares Mechanical Engineering,* Vol. 20, No. 4, (2020), 999-1009.

18. "NACA 0015 Airfoil", In UIUC Airfoil Coordinates Database (Accessed on 2020, August 10) Retrieved from https://m-selig.ae.illinois.edu/ads/coord/naca0015.dat

19. "Wing", In Wikipedia (Accessed on 2020, August 10) Retrieved from https://en.wikipedia.org/wiki/Wing

20. "Airfoil", In Wikipedia (Accessed on 2020, August 10) Retrieved from https://en.wikipedia.org/wiki/Airfoil

21. Zhao, Y., Chen, Y. and Zhou, Y., "Novel mechanical models of tensile strength and elastic property of FDM AM PLA materials: Experimental and theoretical analyses", *Materials & Design,* Vol. 181, (2019), DOI: 10.1016/j.matdes.2019.108089.

22. Perkowski, C., "Tensile-Compressive Asymmetry and Anisotropy Of Fused Deposition Modeling PLA Under Monotonic Conditions", Master Thesis submitted to University of Central Florida, (2017), Retrieved from https://stars.library.ucf.edu/etd/5576.

23. Sri Harsha, A. and Vikram Kumar, C., "Fused Deposition Modeling Using 6-Axis Industrial Robot", Advances in Additive Manufacturing and Joining, Lecture Notes on Multidisciplinary Industrial Engineering, Springer, Singapore, (2020), DOI: 10.1007/978-981-32-9433-2_13.

Persian Abstract

چکیده

مدل‌سازی رسوب (Fusion (FDM یک فرآیند تولید مواد افزودنی برای ساخت اشیا سه بعدی D۳ در یک صفحه افقی از پایین به بالا است. در فرآیند متداول FDM، چاپ اشیا cur منحنی باعث اثر راه پله می‌شود و منجر به پایان ضعیف سطح می‌شود. در این کار، از فرآیند FDM یکپارچه شده با یک ربات DOF Industrial-٦ برای چاپ اشیا cur منحنی با ایجاد مسیرهای ابزار غیر خطی استفاده می‌شود تا از اثر پله جلوگیری شود. یک بال هواپیمای استاندارد NACA 0015 که دارای سطوح منحنی است بدون اثر راه پله با سرعت رسوب یکنواخت با استفاده از یک ربات صنعتی چاپ می‌شود. بال به صورت محدب یا مقعر به لایه‌های منحنی متحدالمرکز تقسیم می‌شود. یک روش جدید با ترکیب مسیرهای ابزار غیر خطی با تغییر جهت اکسترودر برای چاپ اشیا cur منحنی در یک رسوب یکنواخت و بدون اثر پله‌ای ایجاد شده است. از نرم‌افزار شبیه‌سازی ABB Robotstudio برای شبیه‌سازی فرآیند چاپ استفاده می‌شود و نتایج شبیه‌سازی با چاپ بخشی از بال با استفاده از ربات Industrial با اکسترودر FDM به عنوان اثر نهایی تأیید می‌شود. نتایج تجربی نشان داد که بال هواپیما با رسوب یکنواخت با سرعت ثابت و بدون هیچ‌گونه اثر پله‌ای با موفقیت چاپ می‌شود.